Transactions of the Institute of Measurement and Control 26, 2 (2004) pp. 119–137

Machine vision using image data feedback for fault detection in complex deformable webs

Umer Farooq, Tim King, P. H. Gaskell and N. Kapur

University of Leeds, School of Mechanical Engineering, Leeds LS2 9JT, UK

Complex deformable webs like lace fabrics are amongst the most complicated materials to be inspected without any human intervention. The ability of such webs to deform easily, along with their complex patterns, presents a challenging problem for any machine vision system. Their pattern complexity makes it very difficult to use any global image processing or rule-based techniques for inspection, leaving direct comparison with a perfect prototype as the only choice available. Due to the elastic nature of the lace fabric, small distortions are characteristic of the product and are unavoidable. This renders sensitive direct comparison methods, such as those employed for the automatic inspection of printed circuit boards, prone to unacceptable false alarms. In the present work, the authors have exploited a mechatronic methodology, coupled with image processing techniques, to develop a high-speed inspection station for complex patterned lace webs.

Key words: automatic inspection; fault detection; feedback; image processing; lace fabrics; machine vision.

1. Introduction

Work on automating the inspection of lace using machine vision dates back at least as far as 1988 when Norton-Wayne *et al.* (Norton-Wayne, 1991; Sanby *et al.*, 1995), started working on a project supported by the British Lace Federation. They developed a system using direct comparison of a live image with a perfect prototype, which has been commercialized by Shelton Vision Ltd. However, their

Address for correspondence: Umer Farooq, School of Mechanical Engineering, University of Leeds, Leeds LS2 9JT, UK. E-mail: texuf@leeds.ac.uk

 10.1191/0142331204tm112oa

system is designed for finding defects on the lace-knitting machine where the lace is under controlled tension and advances slowly (3 mm/s) giving more processing time. It does not take into account the normal distortions in finished lace. Yazdi and King (King, 1995; Yazdi and King, 1998; Yazdi, 1999) later worked on automating the final inspection stage of lace manufacturing, which demands higher processing speed and process flexibility in terms of different distortions in the lace. They managed to show a system detecting obvious faults, but the speed was low – an inspection rate of only 50 mm/s was reported.

Automatic inspection of lace is particularly challenging because of the very nature of the knitted lace fabric – characterized by its high stretchability, low weight per unit area, low dimensional stability and unlimited design possibilities.

The many design possibilities and the open structure of the lace make it almost impossible to apply global techniques of image processing, such as thresholding, Fast Fourier Transform (FFT) spectrum analysis, edge detection, etc., on their own to trace the defects. Some researchers have successfully used FFT to characterize textural features, like beauty, comfort, transparency, light sensation and lacunarity of 29 different kinds of lace (Mori and Endou 1999, 2001): however, these parameters still remain 'global features' and cannot be used effectively to determine individual defects in the lace to be inspected.

Previous research has indicated that some form of direct comparison of the lace being produced and a reference image is unavoidable. However, the repeats in lace fabric are never identical. This is due to the openness of the structure of lace fabric making small distortions inevitable, moreover, the fabric comprises fine and complex yarn structures, which are easily deformable and are dissimilar in their own. A sensitive direct comparison method, such as that employed for automated inspection of printed circuit boards, will therefore be prone to unacceptable false alarms. Effective subtraction of the image of the lace being inspected and the reference can be achieved only when the two images have the same *size* and *orientation*. In this case, both 'random defects' such as holes, missing threads, etc., and 'geometric defects' such as stretch, skew, etc., will be detected.

For this purpose, a mechatronic approach has been designed. This paper presents a system that uses a 'visual feedback' approach, which minimizes computation and improves robustness in correlation-based tracking by adjusting image rotation, scale and translation parameters in a feedback control mode, to reduce the false alarms and hence detect the lace defects effectively.

2. Experimental rig

The authors have developed an experimental rig that employs five Texas Instruments TMS320C4x series digital signal processors (DSPs) and other necessary machine vision tools to achieve the inspection task in real time. Figure 1 shows the basic processing architecture of the rig, while Figure 2 shows a schematic diagram of its physical arrangement.

The lace is mounted on a transparent drum and is back-lit. The speed of the drum and hence the lace is controlled manually by adjusting the drive frequency to the stepper motor running the drum. An optical encoder is provided to

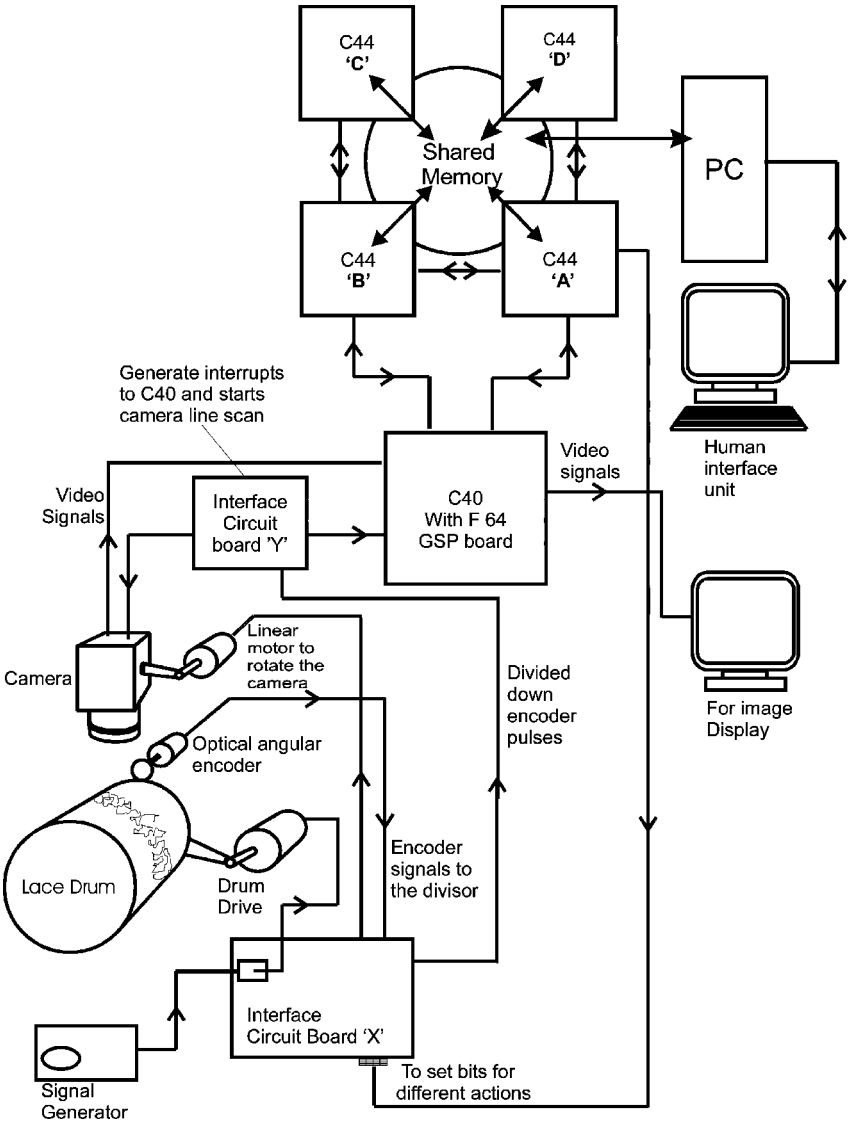

Figure 1 Basic processing architecture of the test rig

synchronize camera line capture with the rotation of the drum. The image is acquired using a DALSA 2048 pixel monochrome line-scan digital CCD camera. The image capture and initial image processing is accomplished using a Coreco Oculus F/64 board (based on a TMS320C40 DSP). The major real-time digital image processing tasks and necessary hardware control are entrusted to a Loughborough Sound Images Digital Signal Processors board PCI/C44S, which is built around four Texas Instruments' TMS320C44 DSPs – 32-bit floating point DSPs optimized for parallel processing. These DSPs have a shared memory that

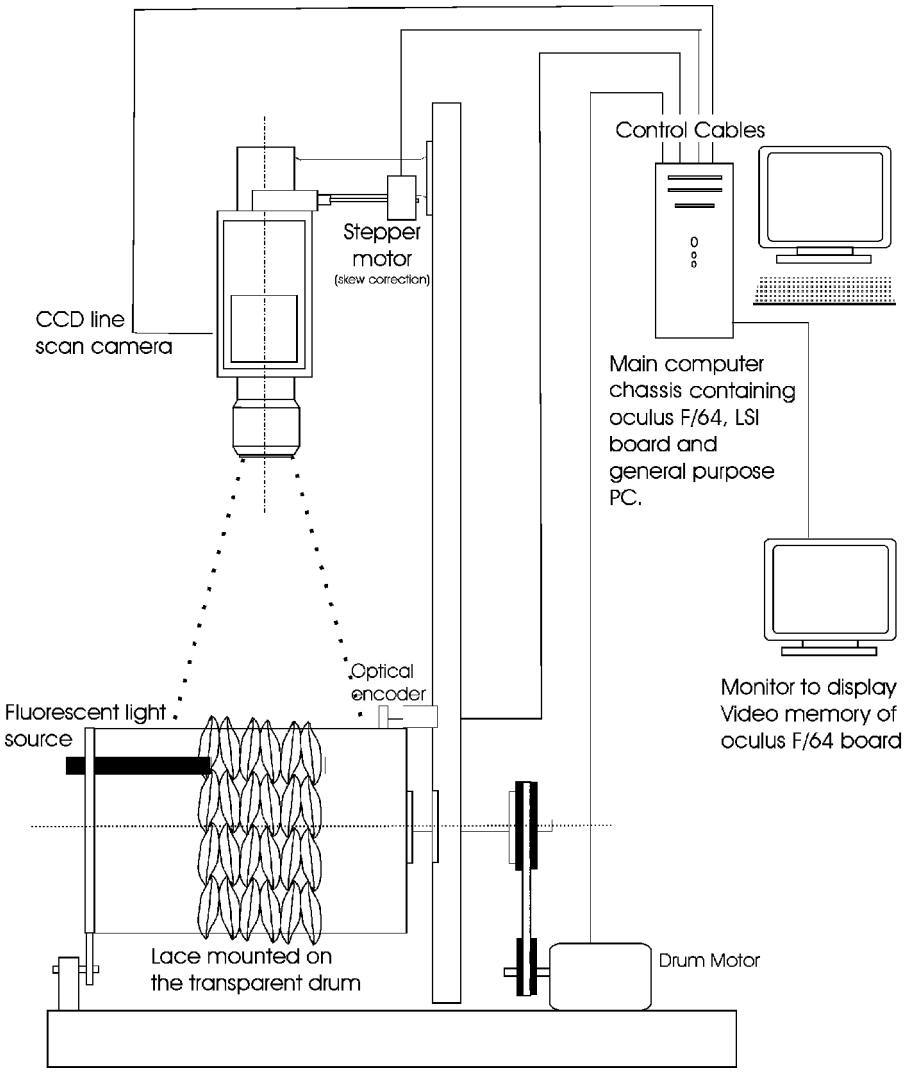

Figure 2 Schematic diagram, showing the physical arrangement of the test rig

also links them to the main PC for necessary human interface. A separate monitor is connected to the Oculus F/64 to display the images acquired by the camera. Two multipurpose interface boards (interface circuit board X, and interface circuit board Y in Figure 1) are also provided.

The optical angular encoder incorporated with the drum produces pulses as the drum rotates. These pulses form an input to a digital divider in interface board A. The numerical divisor is set by the user through DSP C44 A comport. The divided pulse train is fed to the interface circuit board B, which, for each pulse, 1) sends a signal to the camera to take a line and 2) generates an external interrupt to DSP C40

to register a line. These external interrupts allow the system to keep track of the memory where the camera lines are being placed in the Video RAM of Coreco Occulus-F64 board. A change in the divisor will result in a change of longitudinal resolution (camera lines per unit length).

The Coreco Occulus F/64 board is equipped with a TMS320C40 DSP as well as a graphic signal processor (GSP) and plays an important role, not only in capturing and displaying the lace image, but also in performing some initial basic image processing and co-ordinating with processors C44 A and B for subsequent processing. In order to minimize the time involved and to make the system work more efficiently, the lace images are processed in two halves, i.e., the right-hand side of the image is always processed by the C44 A and D, while the left-hand side is handled by C44 B and C.

The camera is mounted to a rotational axis connected via a radius arm to a linear stepper motor, which can control its angle with respect to the drum. The linear sensor of the camera is nominally parallel to the rotational axis of the drum and the camera rotation stepper motor can adjust this alignment to rotate the acquired image slightly. For small angles of rotation, this provides a reasonable approximation to shearing or 'skewing' the lace image. This facility is used to correct any skew or change in orientation detected in the live lace image as explained in the sections to follow.

3. The inspection algorithms

The inspection algorithm comprises two distinct stages, namely the initialization stage and the tracking and inspection stage. The initialization stage involves loading a perfect prototype image of a single pattern repeat of the lace pattern to be inspected and doing first-time synchronization of the live lace image with this perfect prototype (or reference) image. The second stage of tracking and inspection forms the heart of the system, involving a line-by-line tracking of the live lace image with reference to the perfect prototype, subsequent adjustment of the live image lines to correct any lateral, longitudinal or skew distortions and, then, subtraction of the conditioned live image from the perfect prototype. This is followed by a custom-designed morphological erosion filter to remove any residual noise from the subtracted image and detect actual defects.

3.1 Initialization stage

From the outset, it was decided to adopt a direct comparison approach; therefore the first step is to generate a reference image of the lace, which serves as the perfect prototype to be compared with the live image acquired during inspection. Obviously, the reference image should be free of any faults. It should be exactly one pattern repeat, so it can be used cyclically as an endless 'perfect' lace to be referred to throughout the inspection process. Lace designs are made using computer-aided design (CAD) facilities and then fed to modern knitting machines where the needle movements are decided accordingly (Spencer, 1983; Jayaraman,

1995). Because of the nature of the textile material involved, i.e., delicate yarns coupled with complex knitting conditions, the actual lace pattern produced differs in small but significant ways from the CAD pattern. It would also be very difficult to render a CAD-generated synthetic lace image to match real three-dimensional lighting effects at the inspection station. Therefore, the CAD data is not used as the reference prototype. Instead, the initialization stage requires a defect-free lace section to be scanned so as to register a perfect prototype repeat. The second task performed at this stage is the determination of the initial reference position (starting position) of the lace pattern under the camera with respect to the reference image.

3.1.1 Pattern recognition: The two key tasks of the initialization stage, namely to register a perfect prototype repeat and find the initial reference position of the lace under the camera, represent a typical problem of pattern matching. There has been intensive research in the area and a number of methods have been put forward, which can broadly be divided into 1) template-matching techniques, and 2) syntactic or rule-based approaches. Template-matching techniques use the grey levels themselves or derived functions to describe the images. One of the images – usually the known pattern/object model – is chosen as the template, which is then checked against all possible positions in the given image using a raster scan methodology, with the position of the greatest match taken to be the position of the object. As grey-scale values represent pixel intensities, cross-correlation algorithms have difficulty coping with changes in the appearance of features in images. Another problem associated with correlation techniques is that the algorithm is not sensitive in locating the exact 'geometric' shape of the object. The syntactic or rule-based approach, on the other hand exploits the possibility of defining complex objects using a small set of simple sub-patterns or primitives, and some structural rules. It is similar in many aspects to alphabets forming words and then words joining in a various ways, following the grammatical rules, to form phrases and sentences. Here the patterns to be inspected are divided into their simplest primitives and the necessary rules and grammar described to make a valid pattern. During inspection, the algorithms do the *spell* and *grammar* check to detect any defects. Clearly this approach does not require any reference image and can tolerate hostile inspection conditions; however, the objects to be inspected have to be well defined and capable of being 'translated' into distinct and manageable primitives, and structural rules.

Amongst the pattern-matching techniques, the most attractive seems to be a syntactic or rule-based approach, as it can accommodate any distortions in the pattern to be inspected without much trouble. Such techniques are successfully applied to printed circuit boards (Yu et al., 1998). However, defining a set of rules that would encompass the huge range of complex patterns encountered in lace is a Herculean task.

Therefore, the only practical option left is to employ a template-matching technique involving a pixel to pixel correlation between the image of the lace to be inspected with that of a perfect prototype. Since binary images are used due to

intrinsic nature of the lace, the problems associated with grey-scale correlation algorithms can be avoided, and there will be no need of normalization. For binary images, the correlation function is essentially the result of a logical exclusive OR (XOR) between the template and the image under investigation.

The binary correlation can be expressed mathematically by,

$$B_c(x,y) = \sum_{k=1}^{m}\sum_{l=1}^{n} \overline{g(k,l) \oplus f(i+k, j+l)} \tag{1}$$

where $g(k, l)$ is the template (reference) image of size $m \times n$(width $\times$ height), $f(i, j)$ is the image in which the match is to be found, often known as region of interest (ROI) of size $w \times h$, such that $w > m$ and $h > n$. $B_c(x, y)$ is the binary correlation coefficient at position (x, y), where $x = 0,1,2,3 \ldots (w - m) + 1$, and $y = 0,1,2,3 \ldots (h - n) + 1$, unless arrangements have been made for wrapping (or repeating) the reference image. The symbol $\oplus$ represents the binary XOR operation, while the bar sign represents the logical negation function. The x and y that maximize the function in Equation (1) will give the best match between the template and the ROI. The function in Equation (1) is, however, computationally very expensive, for instance, if the ROI has a size of 256×500 and the template is 160×200 the total number of computations will be $160 \times 200 \times (256 - 160) \times (500 - 200) = 9.21 \times 10^8$! An alternative to Equation (1) is finding the x and y that minimize the function,

$$B_c(x,y) = \sum_{k=1}^{m}\sum_{l=1}^{n} g(k,l) \oplus f(i+k, j+l) \tag{2}$$

Theoretically, Equations (1) and (2) both provide the same result. However, since in Equation (2) we are finding the values of x, y that minimize the function we can use the technique of early termination, i.e., to abort the operation when the current correlation coefficient exceeds the 'least' recorded so far, to minimize the total number of computations required. Moreover, the authors have used a coarse to fine matching technique to improve the computational time, involving a first scan of template with shifts of 32 pixels along the x-direction per iteration to register the approximate matched location, followed by a second scan with a single pixel shift around the approximate matched location to register the actual matched section.

In order to find the reference repeat length, the system is fed with the visually perfect section of the lace, a certain representative number of lines are scanned and then cross-correlated with the live image taken by the camera, using the above-mentioned algorithm. The line giving maximum correlation plus the number of lines scanned to form the 'template' indicates a repeat length of the pattern. The scanned lines are stored as the 'perfect prototype'. To find the initial reference position, again a certain representative number of lines are scanned to form the template, which is then searched in the reference image to locate the start position.

3.2 Tracking and inspection stage

The tracking and inspection stage can be divided into four subsections, namely, *tracking*, *feedback control loop*, *local correction* and *image subtraction and morphological filtering*.

3.2.1 Tracking: Once the start point is determined and the live image is in synchronization with the reference image, i.e., the processors know which line the camera is about to scan with respect to the reference image, the system is in a position to make a direct comparison of the lace under inspection (called the 'live' lace image from this point onwards) with the reference image. The camera scans a new line into the Oculus F/64 image acquisition board, the new live lace image line is subjected to some pre-adjustments based on information received by the feedback loop (to be discussed later) before being divided into two halves to be processed in parallel by two DSPs, the TMS320C44 A and B (see Figure 1 and 4).

The algorithm on each DSP takes a section of the live line, for tracking, from around a predefined location called the *nominal track* path. This section is searched in a region consisting of three consecutive lines in the reference image using the binary cross-correlation algorithm discussed in the previous section. The three consecutive lines are: 1) the next logical line in the reference image, 2) the line before it (i.e., the 'corresponding line' for the previous 'live line') and 3) the line after. The algorithm gives the best-matched 'corresponding line' and the best-matched pixel position across the width, for each of the left- and right-hand sides of the image. The best-matched 'corresponding line' helps to compensate for any longitudinal deformation in the live image. For instance, if the 'corresponding line' is the next logical line in the reference image the 'reference image pointer' will 'STEP' one line for the next scan; if the 'corresponding line' is the line before the logical one, the 'reference image pointer' will 'STAY' as it is for the next scan and finally if the 'corresponding line' is the one after the logical line the, the reference image pointer will 'SKIP' one line for the next scan, hence effectively shrinking the live image if it is too big and vice versa. To compensate for the rapid changes in the reference image pointer due to defects in lace or poor correlation during tracking, the movement of the pointer is damped using the following rule:

Consecutive *stay* or *skip* will be replaced by a *step*.

This part of the tracking routine is referred to as Stay−Step−Skip (SSS) routine, and is found to be very effective (see Results and Discussion).

3.2.2 The feedback loop: The SSS routine takes into account both positive and negative longitudinal stretch in the lace being inspected; however, it does not cater for other possible deformations that can make direct comparison of the live lace image with the reference very difficult. These are: lateral offset, horizontal stretch and skew. The authors have developed a novel *feedback loop* approach to align further the live lace image with the reference image and make direct comparison possible. The tracking routine not only gives information about the best 'corresponding line', i.e., the longitudinal position in the reference image, but also about the best-matched horizontal pixel position. The best-matched horizontal pixel positions thus forms the *actual tracked path* as indicated in Figure 3. The difference between the actual tracked path and the nominal tracking path provide us with the right and left *offset*, represented by OS_R and OS_L in Figure 3. The distance between the right and the left actual tracked paths gives an indication about the width of the lace. This information is fed back to the DSP on Oculus F/64 board where

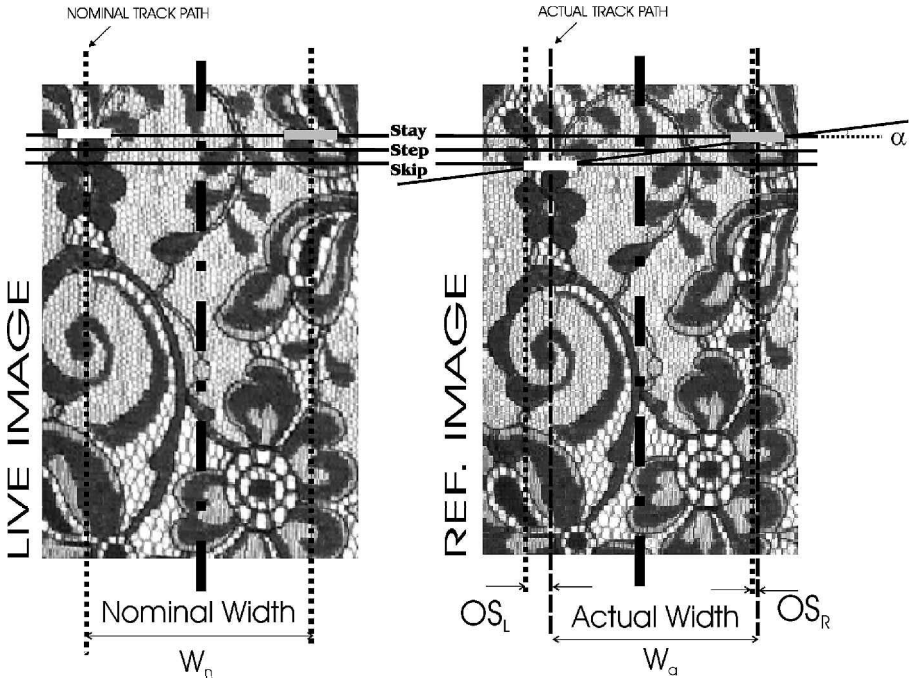

Figure 3 The tracking routine

the next live line is adjusted accordingly. The offset is corrected by shifting the centre, i.e., by altering the number of pixels to left- and right-hand processors. The width is corrected by re-scaling the *live* image before it is divided into two halves. Finally, the two longitudinal positions for the left- and right-hand side of the image give information about the skew angle, α, as shown in Figure 3. We have used a mechatronic approach to correct the skew. The camera is mounted on an axis that can be rotated by a stepper motor (Figures 1 and 2). The skew angle is calculated for every new line scanned and the camera motor driven the correct number of steps in the desired direction, hence scanning the lace at an angle equivalent to the skew. Figure 4 shows the feedback loop and the tasks accomplished by different DSPs. Refer to the Results and Discussion section for results of the feedback approach.

3.2.3 Damping the track path: The tracking path can be adversely affected by any sudden change in the live image section being used for tracking. For instance, the presence of a hole or any major defect in the live image region can cause the binary cross-correlation algorithm to register a maximum correlation at a spurious location. This will result in faulty feedback parameters with the possibility of the inspection run failing. The authors have used a first-order infinite impulse

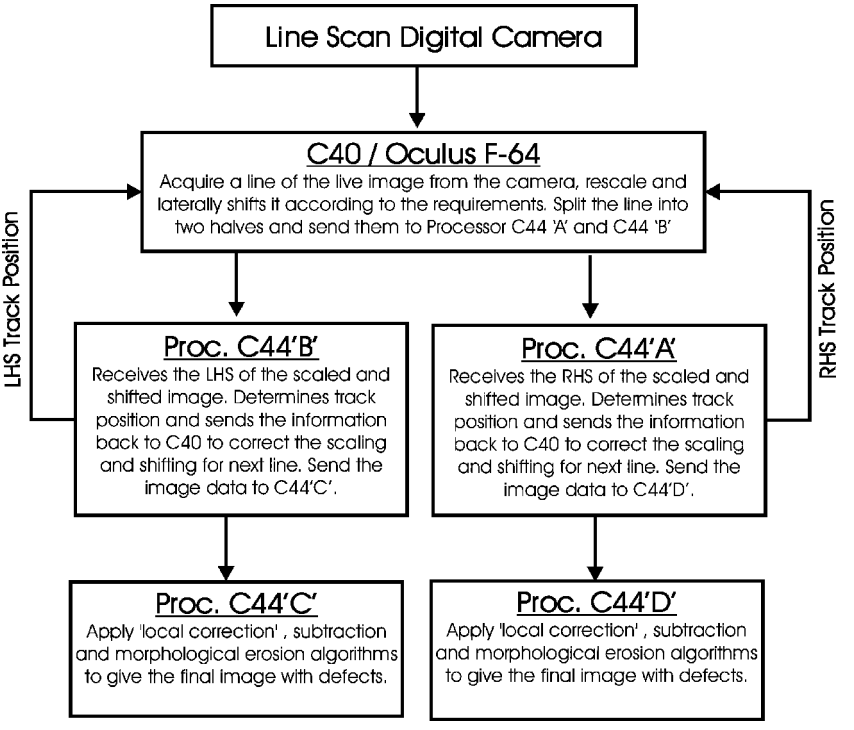

Figure 4 Functional diagram of different processors including feedback loop

response filter (IIR) to smooth the tracked path and avoid possible abrupt deviation in the path due to defects in the lace under inspection.

The basic equation of an IIR filter is shown below:

$$y(n) = \sum_{i=0}^{n} a(i)x(n-i) - \sum_{i=1}^{n} b(i)y(n-i) \tag{3}$$

where n represents the order of the filter, $a(i)$ and $b(i)$ terms represents the coefficients of the filter, $y(n)$ is the output and $x(n)$ the input. The first order IIR filter is implemented on the rig by the following algorithm:

$$\begin{aligned} \textit{Horizontal Position} &= \textit{History\_coeff (Previous H.Position)} + \textit{Curr\_coeff(Current H.position)} \\ \textit{Previous H. position} &= \textit{Horizontal Position} \end{aligned}$$

Where *History_coeff* and *Current_coeff* range from 0 to 1, and always sum to 1.

In the current project the *History_coeff* is kept at 0.707 while the *Current_coeff* is 0.293.

Figure 5 shows the tracked path offset with and without the damping; clearly the damped path is smoother and more reliable than its counterpart. Note that the tracked paths shown in Figure 5 are without any feedback loop.

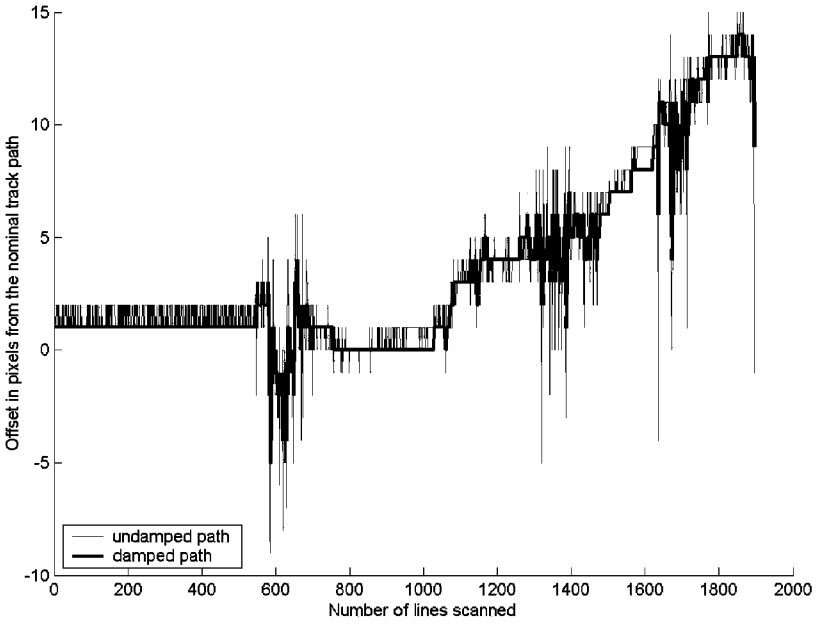

Figure 5 The tracked path offset with and without damping

3.2.4. Local correction: The results from the feedback control loop are very promising (see Results and Discussion). However, since the structure of the lace is very limp and the fabric can easily distort locally, it was found that a localized correlation between the live image and the reference is needed if smaller defects are to be located. This is achieved by dividing the live image line into sections of 32 pixels and searching for their best match in the corresponding region of the reference image. The best-matched section of the reference image is then subtracted from the live image to provide the information about defects.

3.2.5 Subtraction and morphological filtering: The live image is now fully conditioned – well aligned with the reference image and ready to be subtracted from the corresponding section in the reference image to pick up anything which is not the same in the two images (since the images are binary an XOR suffices for this operation). The subtracted image now clearly reveals the defects but it is still accompanied by some noise or 'ghost' image. To remove the remaining noise and hence obtain a defect-only image, suitable morphological filters, e.g., erosion and dilation, are applied to the subtracted image (Serra, 1994; Davies, 1997). To maximize parallel processing capabilities, the morphological filters are applied on the remaining two processors on the LSI board. Binary erosion is defined as:

$$A\Theta B = \{\lambda | B_\lambda \subseteq A\}$$

This means that erosion of a binary image $A(i, j)$ by a binary image B (structuring element) is 1 at a pixel λ if and only if every 1 pixel in the translation of B to λ is

also 1 in B (Bassmann and Besslich, 1995). In other words, if the whole of the structuring element (i.e., all the 1s) lies inside a region in the source image, then the selected pixel (λ) in the output image is set to 1.

The size of the structuring element determines the size of the detected defects. The smaller the structuring element the more sensitive the system. Presently we are using a 3×3 pixel structuring element as reducing it further results in excessive false alarms.

Morphological filters are essentially applied on two-dimensional images. In the present project the data is processed on a line-by-line basis, therefore the authors have devised a tailor-made erosion algorithm. A first-in first-out buffer is created to hold the last three lines of the live image to be filtered. The key points of this algorithm are highlighted below:

1. The three lines are ANDed together to give the resultant line as shown in Figure 6.
2. A window is scanned over the ANDed result, moving one pixel at a time. Three consecutive 1s in this scan indicates that the structuring element of 3×3 pixels lies inside the region, and hence the pixel in the final image should be a 1. The structuring element can easily be changed by increasing the size of the buffer.

The section below shows some of the interesting results recorded using the inspection methodology highlighted above.

4. Results and discussion

The following measures were selected to investigate the effectiveness of different stages of the feedback algorithm:

- *The average offset from the nominal tracking path (Avg. offset)*. This records the deviation in pixels between the actual tracked path and the nominal tracking path. With the feedback loop correcting the position of every new live image line scanned before the tracking, it is expected that the average offset will approach zero as the tracking progresses.
- *The standard deviation of the average offset value in pixels (SD)*. This is a measure of the variation of offset values about zero, and is expected to diminish with the feedback loop active.

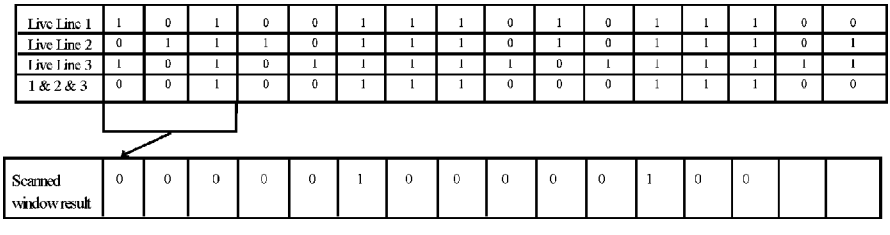

Figure 6 Line-by-line binary erosion algorithm

- *The range of the average offset values in pixels (Range)*. With the feedback loop working, we expect the actual tracked path to follow the nominal tracking path as closely as possible and hence the range should be minimum.
- *The subtracted residue percentage (Sub. res. %)*. The 'conditioning' of the live image is intended to orientate it as closely as possible to the reference image before doing the subtraction, in order to detect any defects. Therefore, the most direct measure of the effectiveness of the feedback algorithm is the amount and nature of noise or residue left when the 'conditioned' live image (with normal generalized distortions but without local defects such as holes) is subtracted from its perfect prototype. The residue in the subtracted image should be minimum and should consist of sparsely distributed pixels. A cluster of pixels indicates, either a defect or insufficient correction of the live image before subtraction. The authors have divided the subtracted residue from the final stage of the inspection algorithm into six categories: clusters with two, four, nine, 12, 16 and 20 pixels, to detect the minimum size of detectable defects.

Three different lace samples (about 500 mm long and 250 mm wide) were inspected. Results are presented in Table 1. Figure 7 shows the lace patterns used in the study.

The standard deviations of the average offset from the nominal position and their ranges are very high for the samples without any correction. Figure 8 shows the average offset readings for sample A without any correction. The massive variation clearly indicates that such a live image cannot give reliable results when subtracted from the reference. Figure 9 (left) shows the result of subtracting this live image with the reference followed by morphological erosion of the same. The live image is not coinciding with the reference image resulting into a subtracted image full of noise. Figure 9 (right) indicates the result of subsequent erosion. The eroded image is giving no information about the possible faults in the fabric.

The standard deviation and the range of the offset path gradually improves as different stages of the feedback correction loop are implemented, with standard deviation reducing to less than one and range well within 10 pixels. Figure 10 shows the offset paths at various stages for sample A: note that with full feedback loop the effective range is less than three pixels once the system is settled. This helps in dynamically reducing the search window size and hence reduces computation time. The massive improvement in the results compared with the raw live image indicates how well the live image is oriented to make it coincide as closely as possible with the reference image.

Figure 11 (left) shows the subtraction of the live image and the subsequent erosion of the resultant image when both the longitudinal correction (SSS routine) and the feedback routine were used to align the live image lines with the corresponding reference image lines. The two images being subtracted are well aligned in this case and resulted into a much better subtraction with less noise. Figure 11 (right) shows the result of applying binary erosion on Figure 11 (left). The defects are clearly recognizable; however there is still some noise, which can result in false alarms.

Table 1 Results from three different lace samples, showing the effectiveness of inspection algorithm

	SAMPLE A				SAMPLE B				SAMPLE C			
	Avg. offset (Pixels)	SD (Pixels)	Range (Pixels)	Sub. res. %	Avg. offset (Pixels)	SD (Pixels)	Range (Pixels)	Sub. res. %	Avg. offset (Pixels)	SD (Pixels)	Range (Pixels)	Sub. res. %
Uncorrected	3.11	17.03	62	29.06	0.70	14.23	61	36.66	0.374	14.436	60	41.14
With SSS only	5.77	7.46	42	26.2	− 10.9	4.19	18	30.21	3.1	2.49	20	35.03
With SSS & offset correction	− 9.63	2.54	21	25.66	− 7.71	1.43	15	29.5	− 9.51	2.04	23	35.77
With full feedback correction	0.056	0.96	10	8.83	0.792	0.49	8	11.43	0.45	0.88	8	16
With additional local correction				5.04				7.25				9.02

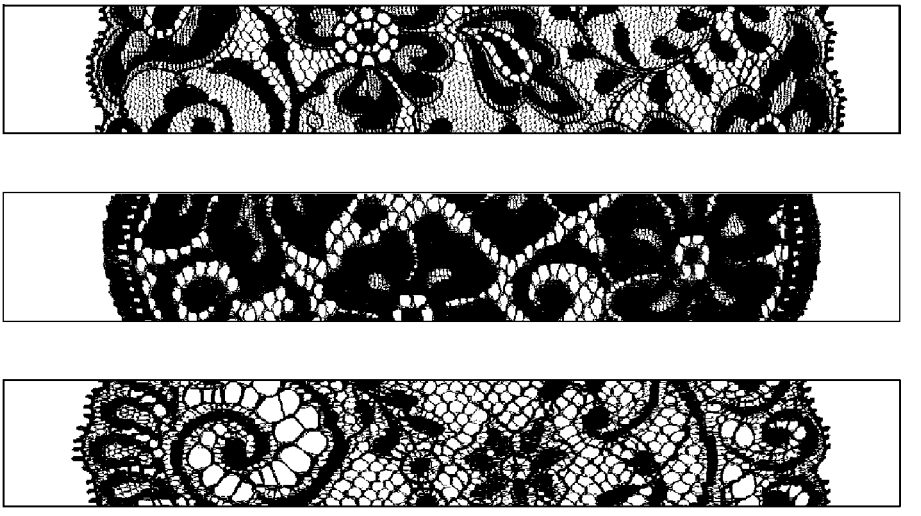

Figure 7 The three lace patterns used in the study; from top to bottom, sample A, B, and C

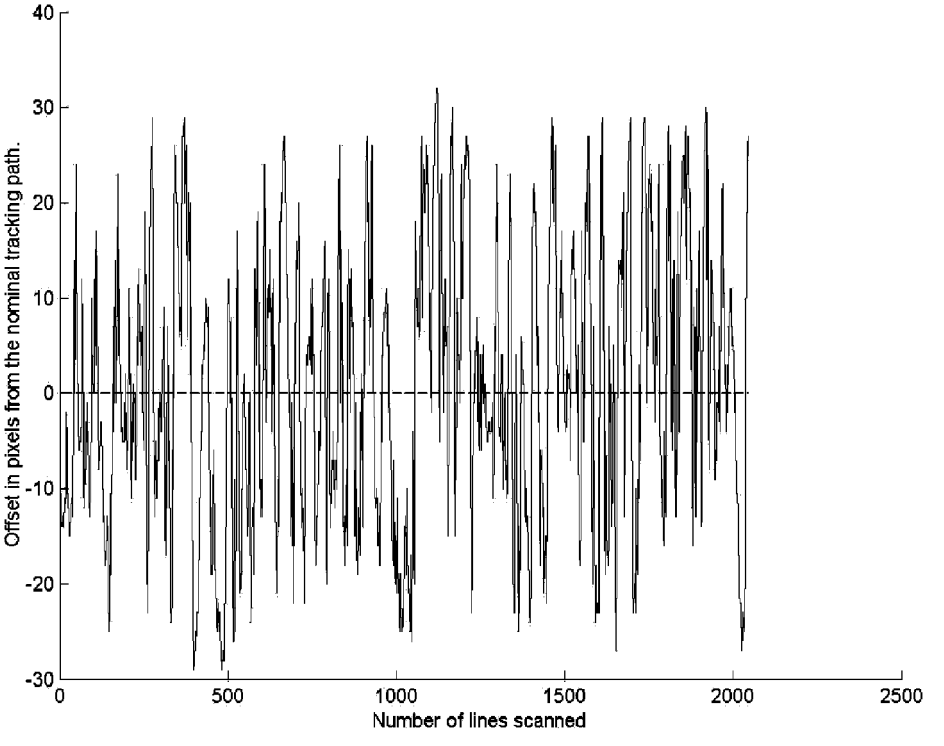

Figure 8 Fluctuations in average offset when the live image is not corrected (sample A)

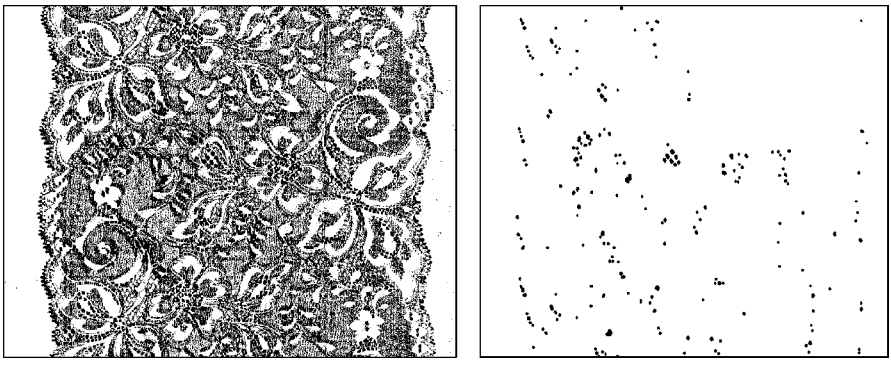

Figure 9 (Left) Live image subtracted from corresponding reference image without any correction; (Right) applying morphological erosion on the subtracted image (left) with a structuring element of 3×3 pixels

Figure 12 shows the result of implementing the local correction routine. The results are very promising, as indicated by the reduction in the noise level in Figure 12. The subtracted image now has a low level of noise, which can easily be removed by applying the morphological filters discussed earlier. The defects are highlighted in the eroded image on the right side.

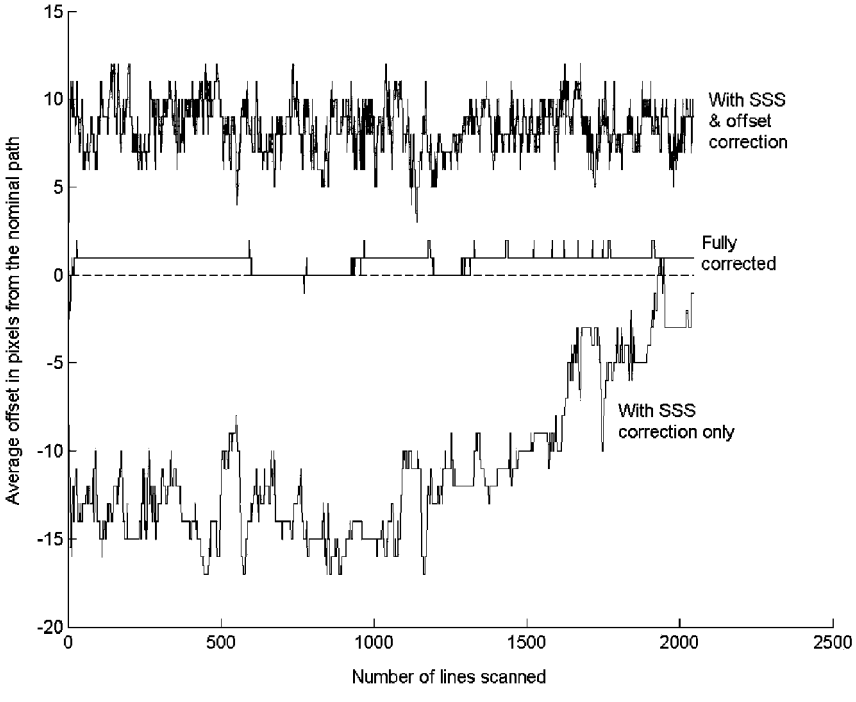

Figure 10 Fluctuations in average offset path at various stages of inspection routine (sample A)

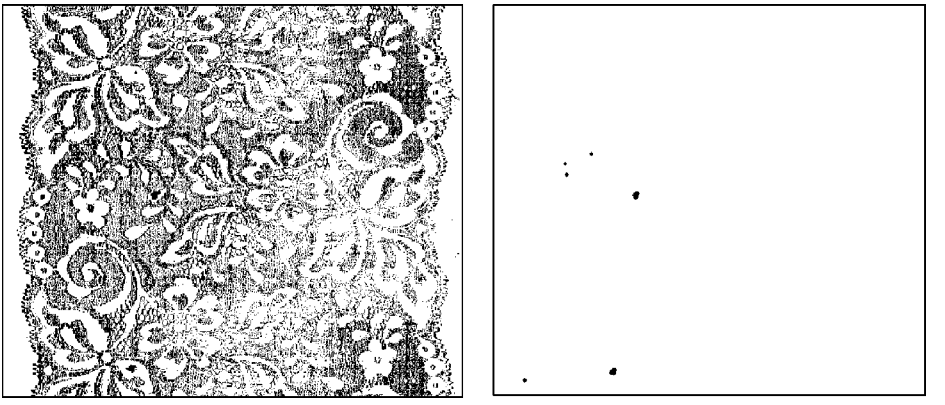

Figure 11 (Left) Subtraction of live image with corresponding reference image with the longitudinal correction (SSS) and feedback control loop implemented. (Right) Applying morphological erosion on the subtracted image (left) with a structuring element of 3×3 pixels

The column headed Sub. res. % in Table 1 indicates the percentage of pixels left as noise after the subtraction operation (the number of black pixels in Figures 10, 11 and 12). As expected, the number of such pixels falls sharply as the live image lines are oriented more closely to the reference image lines after the implementation of different stages of the inspection algorithm. As indicated earlier, if the live image is well aligned with the reference image, the subtracted image residue should be minimum and sparsely located. A defect in the live image can then

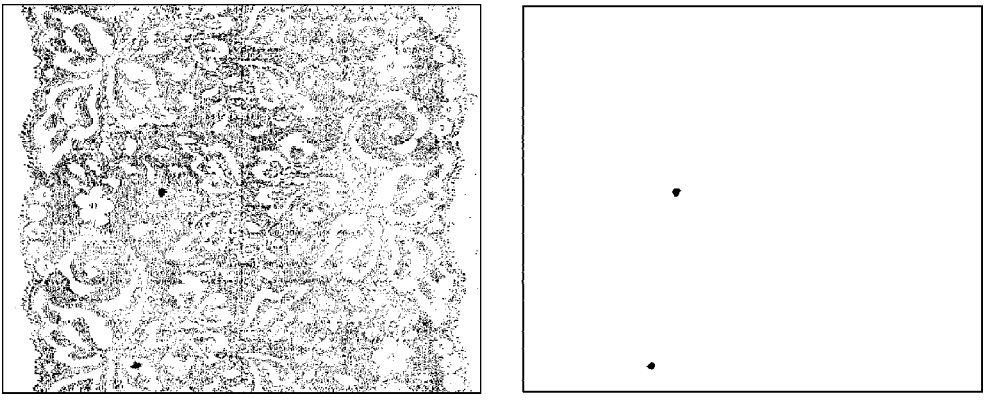

Figure 12 (Left) Subtraction of live image from the corresponding reference image with the longitudinal correction (SSS) and feedback control loop and local correction routine implemented. (Right) Applying morphological erosion on the subtracted image (left) with a structuring element of 3×3 pixels.

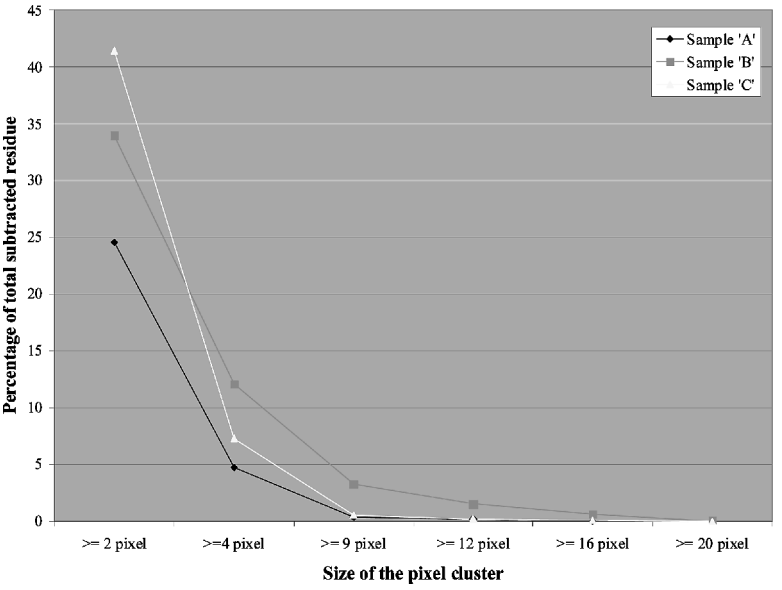

Figure 13 Cumulative frequency curves for different cluster sizes present in the subtracted residue from the final stage of inspection routine, i.e., the local correction

be located by recognizing a cluster of residue pixels using morphological techniques. The size of the defect that can be successfully detected depends on the distribution of the subtracted residue. To decide the minimum size of the detectable defect, the authors have tabulated a cumulative frequency curve for different cluster sizes present in the subtracted residue from the final stage (i.e., the local correction stage of the inspection routine), using lace samples with no local defects. Figure 13 shows the result. It can be seen that with all the three samples used there is hardly any cluster bigger than 16 pixels, i.e., a 4×4 pixel box, which is taken to be the minimum detectable defect size. With a resolution of about 0.25 mm per pixel in each direction the minimum detectable defect size is thus 1×1 mm.

5. Conclusion

A machine vision system using an image data feedback loop has made it possible to detect faults in highly flexible and easily distortable textile webs in real time. A direct comparison of the live image of the lace with a perfect prototype reference image, on an incremental, line-by-line basis is adopted. The problem of inherent distortions in the lace, which make direct comparison very difficult and subject to excessive false alarms, is successfully resolved by adjusting the live lace image in real time, using a closed-loop feedback correction routine, before it is compared with the perfect prototype. Each live line scanned provides feedback data to correct subsequent lines. The longitudinal stretch (or shrinkage), is corrected by

controlling the reference image 'pointer'; the lateral distortions are corrected by rescaling each live line's width; the lateral offset is adjusted by shifting the centre of the image and finally the skew or orientation of the lace is corrected by rotating the camera using a stepper motor. The system is performing very successfully and development work is under way to further increase inspection speed. The inspection speed with the current rig is about 44 mm/s. The multi-DSP approach, whilst the only way of obtaining sufficient processing power at the commencement of the project, makes development very difficult. Load balancing is also problematic. The next version of the system will be based on a modern high-performance single processor.

References

Bassmann, H. and **Besslich, P.W**. 1995: *Ad Oculus digital image processing, professional version 2.0*. London: Henning Bassmann, International Thomson Publishing, 231.

Davies, E.R. 1997: *Machine vision, theory, algorithms and practicalities*, 2nd edition. New York: Academic Press, 647–56.

Jayaraman, S. 1995: Computer aided design and manufacturing: a textile apparel perspective. In Acar, M., editor, *Mechatronics in textile design*. Dordrecht Kluwer Publishers, 67–74.

King, T.G., 1995: *Mechatronics and Machine Vision for Quality and Efficiency Improvement in Textile Lace Manufacture, Proc. 2nd International Mechatronic Design and Modelling Workshop*, p. 1–9, Metu, Ankara, Turkey.

Mori, T. and **Endou, Y**. 1999: Evaluation of visual texture and aesthetic appearance of lace patterns. *Journal of Textile Institute*, 90 Part 1, 100–12.

Mori, T. and **Endou, Y**. 2001: Fluctuation of lace patterns using frequency analysis. *Journal of Textile Institute* 92 Part 1, 150–56.

Norton-Wayne, L. 1991: Inspection of lace using machine vision. *Computer Graphics Forum* 10, 113–19.

Sanby, C., **Norton-Wayne, L.** and **Harwood, R**. 1995: The automatic inspection of lace using machine vision. *Mechatronics* 5, 215–31.

Serra, J. 1994: Morphological filtering: an overview. *Signal Processing* 38, 3–11.

Spencer, D.J., (1983): *Knitting technology*. Pergamon Press, Oxford.

Yazdi, H.R. 1999: Automatic visual inspection of lace. PhD thesis, University of Birmingham.

Yazdi, H.R. and **King, T.G.** 1998: Application of vision in the loop for inspection of lace fabrics. *Real Time Imaging* 4, 317–32.

Yu, S.S., **Cheng, W.C**. and **Chiang S.C**. 1998: Printed circuit board inspection system. SPIE Vol. 1004, *Automated Inspection and High Speed Vision Architectures II*, 126–34.